iForest
Biogeosciences and Forestry

Research Article
doi: 10.3832/ifor4021-015
vol. 15, pp. 128-132

Can forest trees take up and transport nanoplastics?

Maria Elvira Murazzi [(1)],
Paolo Cherubini [(1-2)],
Ivano Brunner [(1)],
Ralf Kägi [(3)],
Matthias Saurer [(1)],
Paula Ballikaya [(1)],
Frank Hagedorn [(1)],
Maya Al Sid Cheikh [(4)],
Gabriela Onandia [(5-6)],
Arthur Gessler [(1-7)]

Plastic contamination of ecosystems has increased dramatically over the last decades, raising concerns about the negative impacts of plastic particles on aquatic and terrestrial systems. In recent years, the focus of most research has shifted from large fragments (macroplastic) to micro- (<5 mm) and more recently to nano-plastic (<1000 nm) particles as more evidence has come to light about their ubiquity in water, soils, and living systems, and their effects on ecosystem and human health. In this study, we investigate nanoplastic uptake in the roots of seedlings (1-2 years old) of three different tree species and assess their transport to different tissues. Parts of the main roots of silver birch (*Betula pendula* Roth), sessile oak (*Quercus petraea* Matt. [Liebl.]), and Norway spruce (*Picea abies* [L.] Karst.) were immersed for one or four days in a suspension containing ^{13}C-labelled nano-sized polystyrene particles (^{13}C-nPS; 99% ^{13}C, d = 28 ± 8 (1 σ) nm). Carbon stable isotope analysis showed significant ^{13}C enrichment ($P < 0.05$) in the immersed part of the root after one day of treatment in all three species, and after four days in *Q. petraea* alone. Signals of significant ^{13}C enrichment were also found in the aboveground tissues of the trees. The stem of *B. pendula* in particular showed a significant ^{13}C enrichment after one day of treatment ($P < 0.01$). This indicates that nanoplastic particles can be taken up through tree roots into the tree's central cylinder, where they are subsequently conveyed through the tree by acropetal transport *via* the xylem.

Keywords: Forest Trees, Nanoplastic, Polystyrene

Introduction

Plastics are synthetic polymers derived mainly from petroleum. Plastic production rates have increased steadily over the past decades, as have the attendant rates of waste production and pollution (Jambeck et al. 2015, Geyer et al. 2017). A lightweight, low-cost product, plastic is also resilient, durable, and easily transported and is therefore ubiquitous in modern life. The longevity of plastic is also the reason for its accumulation in the environment. Plastics have become a source of pollution affecting almost every ecosystem on the planet.

Plastic pollution is currently a key concern for human society, and its mitigation is a big challenge for future research and policy making (Mitrano & Wohlleben 2020). Plastic litter starts as macroplastics, such as bottles or packaging, which slowly fragment into micro- (<5 mm) and nano-sized particles (<1000 nm – Allen et al. 2019). Such small particles can rapidly disperse across many ecosystems (De Souza Machado et al. 2019). Most studies to date have focused on aquatic systems, such as rivers, lakes, and oceans. However, only about 5% of the annual terrestrial plastic waste ends up in marine ecosystems. The fate of the remaining plastic litter is still largely unknown due to the fragmentation of plastic into nanoparticles (Jambeck et al. 2015, De Souza Machado et al. 2018).

Research has only recently started to focus on terrestrial ecosystems after decades of scrutinizing the fate and impact of plastics on marine and freshwater ecosystems. Microplastics have been found in floodplain soils (Scheurer & Bigalke 2018), agricultural soils (Rillig et al. 2017), forests (Choi et al. 2020), and glaciers (Ambrosini et al. 2019). The range of ecosystems in which these particles are found indicates that micro- and nanoplastics can be transported by wind (Rezaei et al. 2019), and are therefore likely to also contaminate forest ecosystems. Atmospheric transport seems to be the most important pathway explaining the presence of plastic in remote areas and regions worldwide (Dris et al. 2016, Gasperi et al. 2018, Bergmann et al. 2019, Brahney et al. 2020, 2021, Materić et al. 2021). However, the fate of micro- and nanoplastics in the different ecosystems is almost unknown due to the analytical challenge of their detection in the environment (Wagner & Reemtsma 2019, Lehner et al. 2019, Patil et al. 2022).

A current challenge is to understand the micro- and nano-sized plastic pools and fluxes in terrestrial ecosystems, as well as the impact of plastic particles on plants and ecosystem functioning. Microplastics can affect the biophysical properties of soil, but our understanding of the complex relationships between microplastics, soil

(1) WSL Swiss Federal Research Institute, Birmensdorf (Switzerland); (2) Department of Forest and Conservation Sciences, Faculty of Forestry, University of British Columbia, Vancouver BC (Canada); (3) Eawag, Swiss Federal Institute of Aquatic Science and Technology, Dübendorf (Switzerland); (4) Department of Chemistry, University of Surrey, Stag Hill, Guildford, GU2 7XH, Surrey (United Kingdom); (5) Research Platform "Data", Leibniz Centre for Agricultural Landscape Research (ZALF), Müncheberg (Germany); (6) Berlin-Brandenburg Institute of Advanced Biodiversity Research (BBIB), Berlin (Germany); (7) Institute of Terrestrial Ecosystems, ETH Zurich, Zurich (Switzerland)

@ Maria Elvira Murazzi (maria.murazzi@wsl.ch)

Received: Nov 15, 2021 - Accepted: Feb 22, 2022

Citation: Murazzi ME, Cherubini P, Brunner I, Kägi R, Saurer M, Ballikaya P, Hagedorn F, Al Sid Cheikh M, Onandia G, Gessler A (2022). Can forest trees take up and transport nanoplastics? iForest 15: 128-132. - doi: 10.3832/ifor4021-015 [online 2022-04-09]

Communicated by: Werther Guidi Nissim

abiotic properties, microbial communities, and plants is still limited (De Souza Machado et al. 2019, Lozano et al. 2021a, 2021b). Wang et al. (2022) recently found that microplastics affect physical, chemical, and microbiological soil properties and that polymer type, dose, shape, and size can have different impacts in soils. Changes in soil properties may then affect the growth and development of plant roots, with potential consequences for ecosystem functioning.

Microplastics and nanoplastics can be absorbed by plant root hairs (Azeem et al. 2021). Indeed, Bosker et al. (2019) found a germination delay effect following the accumulation of microplastics in the root hairs of cress seedlings. Sun et al. (2020) recently demonstrated nanoplastic uptake in *Arabidopsis thaliana* (L.) Heynh. by root tips and subsequent negative physiological effects. Giorgetti et al. (2020) showed that onion seeds germinating in polystyrene nanoplastic suspensions exhibited decreased root growth and signs of cyto- and genotoxicity. In contrast, experiments with aquatic macrophytes have shown that growth depression only occurs when nanoplastic concentrations in the sediment exceed concentrations unlikely to be found in the environment (Van Weert et al. 2019). Van Weert et al. (2019) used solutions with 0.03, 0.1, 0.3, 1, and 3% nanopolystyrene concentrations, which covers the range of concentrations likely to be found in the environment. An experiment with duckweed by Dovidat et al. (2020) showed that although nanoplastic particles attached to roots, they were not detected within the plant. Li et al. (2020) demonstrated submicrometer plastic uptake in crop plants *via* a crack-entry pathway through roots. In a recent hydroponic experiment, Liu et al. (2022) found evidence of both nano- and micro-plastics uptake in rice seedlings through the roots and subsequent transport to aerial parts. Apoplastic transport was assumed to be the main pathway for plastic particles reaching aboveground tissues. Nanoplastic absorption by roots from colloidal solutions and transport in higher plants (*Murraya exotica* L.) has been shown by Zhang et al. (2019). As with this study, the authors found that transport did not occur in the xylem and instead assumed it to be restricted to the apoplast of the lignified epidermis of roots and stems.

At present, there is a limited understanding of the impact of nanoplastics on tree physiology and forest health, and it is still unclear whether trees are able to take up nanoplastic particles *via* their roots. To assess whether and, if so, to what extent nanoplastics are taken up by trees through their roots, we immersed the roots of seedlings from three different forest tree species in a ^{13}C-labelled nano-sized polystyrene particle suspension (^{13}C-nPS) with a concentration similar to that observed in soils of polluted terrestrial ecosystems (Huerta Lwanga et al. 2016, Windsor et al. 2019). We further investigated whether nanoplastics can be transported to different aboveground tissues.

Materials and methods

Nanoplastic preparation, pre-processing, and characterization

Styrene-$^{13}C_8$ (Sigma-Aldrich, Buchs, Switzerland, ≥99 atom % ^{13}C) was used to synthesize batches of spherical ^{13}C-nPS of 28±8 (1 σ) nm in size following the procedure of Al-Sid-Cheikh et al. (2020). Unreacted monomers were removed by ultrafiltration (exclusion size of membrane: 30,000 g mol^{-1}). The hydrodynamic diameter (z average) of the particles was determined by dynamic light scattering (DLS) on a Zetasizer (Nano-ZS®, Malvern Instruments, UK). Secondary electron images recorded on a dedicated scanning transmission electron microscope (STEM, HD 2700 Cs®, Hitachi, Japan) indicated that the particles were mostly spherical and not aggregated (Fig. S1 in Supplementary material).

Plant material and greenhouse setting

In February 2019, 36 seedlings of three different tree species, previously grown outdoors in a forest nursery, were potted into 12 cm diameter plastic pots with a mixed soil substrate ("Containererde", Ökohum GmbH, Switzerland). One-year-old silver birch (*Betula pendula* Roth), two-year-old sessile oak (*Quercus petraea* Matt. [Liebl.]), and two-year-old Norway spruce (*Picea abies* [L.] Karst.) were used. As each plant was potted, its main root was directed through a central hole at the bottom of the pot so that it was protruding out of the pot. This part of the root was then put into a smaller pot containing the same substrate, beneath the first pot (a sketch of the experiment set-up is shown in Fig. 1a).

This set-up enabled easy access to part of the rooting system for the ^{13}C-labelling procedure (see below). The seedlings were then grown under natural light conditions in a greenhouse. The position of each seedling in the greenhouse was randomly changed once a week, and the pots were watered to field capacity twice a week.

Nanoplastic uptake experiment

At the end of August 2019, the main root of each seedling was carefully removed from the lower pot and rinsed with demineralised water to remove any adhering soil particles. The tips of the main roots (R1) were inserted into 15 ml Falcon® tubes (VWR, Dietikon, Switzerland) containing 12 ml of quarter-strength Hoagland nutrient solution (Fig. 1b). On the same day, ^{13}C-nPS were added to the nutrient solutions of six plants of each species to reach a 0.2% mass concentration (according to Huerta Lwanga et al. 2016). The other six individuals of each species were used as controls. The acropetal part of the main root (R2) that was not immersed in the suspension (Fig. 1b) was covered daily with a fresh wet paper towel to prevent desiccation during the experiment.

For each species and treatment, three seedlings were sampled after one day of exposure to the ^{13}C-nPS. The remaining three seedlings were sampled four days after the ^{13}C-nPS was added. For the four-day-long exposure, the amount of suspension in the tubes was monitored daily and nutrient solution was added as needed to account for evaporation and absorption by the roots.

Plant harvest

After one or four days of treatment, the tips and the rest of the main roots that were immersed in the ^{13}C-nPS suspension, plus a section of the root that was moistened by the suspension (~ 1cm, following Gessler et al. 2002), were collected from each plant (R1 – Fig. 1b). The individual root pieces were washed intensively with demineralised water for five minutes, then dried with a paper towel and weighed using a precision laboratory balance (PM 200, Mettler-Toledo, Columbus, OH, USA). The rest of the plant was subdivided into the following sections (see Fig. 1b): the upper

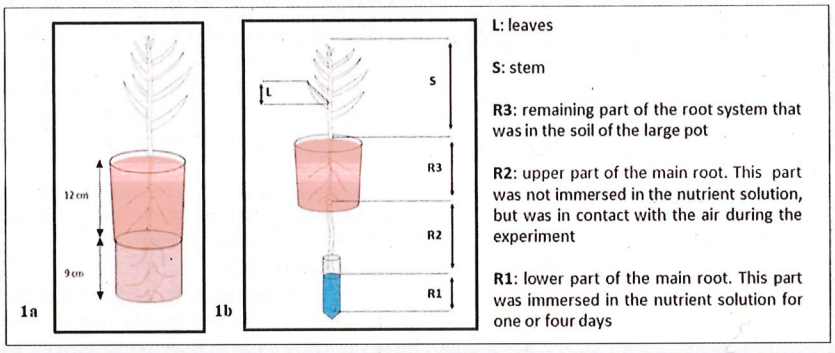

Fig. 1 - Experiment set-up (not to scale). Average stem heights of the different forest tree species were: 18 cm for *Q. petraea*, 20 cm for *P. abies*, and 42 cm for *B. pendula*. (a) Illustration of the potting preparation of a forest seedling; (b) illustration of a seedling during the experimental phase. The five different plant tissues that were analysed are also indicated (R1, R2, R3, S, L).

part of the main root outside of the exposure medium (R2), the remaining part of the root system in the main pot (R3), the stem (S), and the leaves (L). The roots (R3) were washed with tap water to remove adhering soil particles. All sections were weighed to obtain fresh weights, then oven dried at 60 °C for four days to obtain dry weights.

Stable isotope analysis

After drying, each of the five different tissues of the seedlings were homogenized using a ball mill for 1.5 minute at a frequency of 30 cycles per second (MM 400®, Retsch, Haan, Germany). For every tissue, first controls and then treatments were milled to avoid any possible contamination. One milligram of the homogenised material was weighed into a tin capsule then combusted in an elemental analyser (EA-1110®, Carlo Erba, Milan, Italy). The resulting CO_2 was analysed in a coupled isotope-ratio mass-spectrometer (Delta Plus XL®, Thermo, Bremen, Germany). The ratio of $^{13}C/^{12}C$ in the sample indicates its relative deviation in per mil from the international standard, V-PDB, which is given as $\delta^{13}C$. Laboratory standards and international standards with known $\delta^{13}C$ values were used for the calibration of the measurements, resulting in a precision of 0.2‰ for $\delta^{13}C$.

Data analysis and statistics

For each of the different tree species, we calculated the difference in $\delta^{13}C$ between the tissues of the plants treated with ^{13}C-nPS and the control plants. We refer to this difference in $\delta^{13}C$ as $\Delta\delta^{13}C$. Positive $\Delta\delta^{13}C$ values indicate ^{13}C-enrichment in treated plants. We used RStudio Team 2020 to test for the significance of ^{13}C enrichment by performing a mixed analysis of variance (ANOVA), an analysis of variance (ANOVA), and a one-sided *t*-test for each of the five tissues. These tests detect ^{13}C-incorporation in or adsorption to a specific tissue in a specific species and at a specific time. Finally, the ^{13}C mass balance for each tissue in each plant was calculated to quantify the amount of ^{13}C or ^{13}C excess (in g ^{13}C) contained in each tree's compartment (Tab. S1 in Supplementary material).

Results and discussion

The addition of ^{13}C-labelled nanopolystyrene led to a very high enrichment in the incubated parts of the roots (Fig. 2). It also caused a significant overall $\delta^{13}C$ increase in all three tree species, indicating that trees were able to take up nanopolystyrene through their roots and incorporate it in their tissues (ANOVA – Tab. 1).

The part of the rooting system immersed in the polystyrene solution (R1) showed positive $\Delta\delta^{13}C$ values in all three species after both one- and four-day-long treatments ($P < 0.0001$), indicating ^{13}C enrichment (Fig. 2). The ^{13}C enrichment is statistically significant (one-sided *t*-test: $P < 0.05$) in all three species following the one-day treatment,

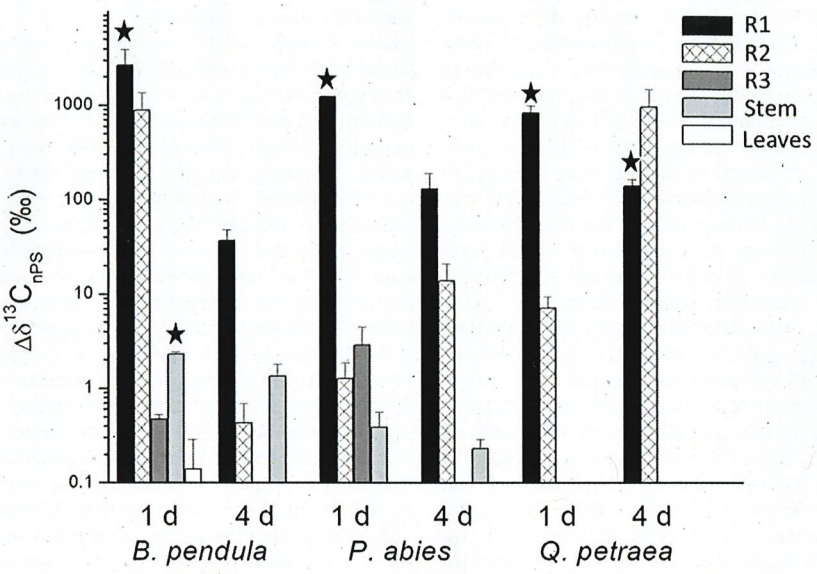

Fig. 2 - Differences in ^{13}C between plants with ^{13}C-nanopolystyrene ($\Delta\delta^{13}C$) and controls. The $\Delta\delta^{13}C$ between the plants treated with ^{13}C-labelled nanopolystyrene and the control plants for various tissues of all three tree species at different times of exposure (1d= one-day treatment; 4d= four-day treatment). Means and standard errors of 3 replicates. Black stars indicate statistically significant differences ($P < 0.05$) between control and treatment, tested by a one-sided *t*-test. (R1): lower part of the main root, which was immersed in the nutrient solution; (R2): upper part of the main root, which was not immersed in the nutrient solution but was in contact with the air during the experiment; (R3): remaining part of the root system that was in the soil of the large pot.

and in *Quercus petraea* following the four-day treatment (Fig. 2). Studies of both freshwater plants and an ornamental shrub have shown that nanoplastics can attach to the root surfaces (Zhang et al. 2019, Dovidat et al. 2020). If the intensive root washing failed to remove all ^{13}C-nPS particles, the enrichment could reflect strong binding to the root surfaces and/or particle uptake via the roots (Sun et al. 2020).

The part of the root not immersed in the polystyrene solution (R2) showed positive $\Delta\delta^{13}C$ values in all three species ($P < 0.01$, Tab. 1) and hence ^{13}C enrichment. Seven out of 18 labelled seedlings showed $\Delta\delta^{13}C$ values > 5‰, which is well above the natural variability of $\delta^{13}C$ in unlabelled seedlings, with a standard deviation of 0.8‰.

In the part of the root system that remained in the soil (R3), the labelling did not change $\delta^{13}C$ values significantly. However, the $\Delta\delta^{13}C$ R3 value of one out of 18 treated *P. abies* seedlings (after one day of treatment) exceeded the standard deviation of control trees, indicating a ^{13}C enrichment (Fig. 2).

Leaf tissues showed significant differences in $\Delta\delta^{13}C$ at the treatment level ($P < 0.05$ – Tab. 1). A slightly positive $\Delta\delta^{13}C$ value was found in *B. pendula* after one day of treatment (0.14 ‰ ± 0.47 – Fig. 2), but this value was not statistically significant.

In stem tissues, $\Delta\delta^{13}C$ values depended upon tree species (treat × species: $P < 0.001$ – Tab. 1). The enrichment of $\delta^{13}C$ in the stems of *P. abies* and *Q. petraea* remained below detection limit, but the stem tissues of *B. pendula* ($\Delta\delta^{13}C$ = 2.28 ‰ ± 0.45)

Tab. 1 - ANOVA testing the effects of exposing three tree species to ^{13}C-labelled nanopolystyrene for one and four days on $\delta^{13}C$ values in various tissues. F-values from ANOVA are shown. (***): p< 0.001; (**): p< 0.01; (*): p< 0.05.

Factor	df	All tissues	Root1 (R1)	Root2 (R2)	Root3 (R3)	Stem	Leaves
Tissue	4	66.8***	-	-	-	-	-
Treat	1	74.8***	178***	8.14**	0.05	2	4.63*
Species	2	4.1*	0.79	0.69	7.8**	6.9**	17.9***
Time	1	8.4**	22.7	0.02	1.3	0.58	0.01
Species × Treat	2	0.6	0.2	0.82	2.15	40.3***	1.41
Tissue × Treat	4	49.2***	-	-	-	-	-

were significantly enriched (one-sided *t*-test: $P < 0.01$) after one day of treatment (Fig. 2), indicating the presence of nanopolystyrene. Estimating the ^{13}C excess according to Ruehr et al. (2009) revealed that this enrichment of *B. pendula* stems represents 0.19% of the total ^{13}C-labelled polystyrene added to the exposure media (Tab. S1 in Supplementary material). This percentage corresponds to the ratio between the average ^{13}C content in the stem tissue ($4.44 \cdot 10^{-5}$ g) and the average ^{13}C content in the incubation solution (0.0232 g). In details, the incubation solution contained 0.0232 g of ^{13}C (12.6 ml, or approximately 12.6 g) solution with a polystyrene concentration of 0.2%. This results in 0.0252 g of polystyrene per incubation vial, with approx. 93% of the molecules consisting of C and 99% labeled with ^{13}C. Thus, the ^{13}C content in the incubation vial is 0.0232 g ^{13}C. Whereas the average ^{13}C content in the stem tissue ($4.44 \cdot 10^{-5}$ g) is the result of the following multiplication: $2.495 \cdot 10^{-5}$ (^{13}C atom% excess equalling the enrichment of 2.28 ‰) · 3.56 g stem tissue biomass (g dry weight) · 0.5 (C content in g C per g dry weight).

The enrichment in the stem may be the result of ^{13}C uptake in the central cylinder of the root and subsequent acropetal transport *via* the xylem. An alternative explanation, as suggested by Zhang et al. (2019), is that ^{13}C-nPS is transported in the apoplast of the lignified root epidermis without crossing the endodermis (and thus without reaching the central cylinder).

The ^{13}C enrichment in the stem of *B. pendula* (Fig. 2) and the overall treatment effect for leaves (Tab. 1) suggests that long-distance transport of nanoplastics from the roots to the shoot occurs in trees. *Betula pendula* is an early successional species with high water use (Leuschner 2002); its transpiration rates are higher than those of the two late successional species studied here (*Q. petraea* and *P. abies*). Xylem transport rates might therefore explain the significant accumulation of labelled ^{13}C in the stems of *B. pendula* but not in the stems of the other two species.

It is important to note that the ^{13}C signal of added nanopolystyrene gets diluted in seedling biomass when transported out of the treated part of the root into the other plant compartments. For example, if one assumes that the majority of the 5% of the label found in the R1 root of *P. abies* after one day of treatment ($\Delta\delta^{13}C$ = 1237‰ ± 19 – Fig. 2) is uniformly transported to R2, R3, and aboveground tissues, this label is diluted by a factor of 0.021 (the biomass of R1 is 2.1% of the biomass of R2 + R3 + S + L; see Tab. S1 in Supplementary material). This would result in an average ^{13}C enrichment of 1.30‰. The ^{13}C enrichment in the stems of *B. pendula* exceeds this value ($\Delta\delta^{13}C$ = 2.28‰ ± 0.45), implying higher uptake of nanoplastics. The ^{13}C enrichment in the root parts R2 and R3 and stems of *P. abies* after one day of treatment is in this range but is not significant due to the high variability among individuals.

Even if signs of ^{13}C enrichment were found in all the tissues, $\Delta\delta^{13}C$ values of the aboveground tissues were close to the detection limit, revealing some discrepancies between the two different exposure times. When comparing the two exposure times, more statistically significant values were found after one day of treatment as compared after four days of treatment. We speculate that nanoparticles change root morphology and functioning over time, resulting in reduced uptake and transport to other tissues. Indeed, Zhang et al. (2019) found that polystyrene nanoparticles created a physical barrier in the root micropores and significant injuries at the epidermal root cell level. We therefore assume that longer incubation times did not lead to higher uptake in our experiment. This does not explain the lower enrichment after 4 days of exposure (found in some cases), but this may be due to the fact that ^{13}C enrichment was mostly close to the detection limit.

In conclusion, the use of ^{13}C-nPS in our experiment gave some first evidence of the potential uptake of nanoplastics in trees. The highest ^{13}C enrichments from ^{13}C-nPS were obtained from roots immersed in the exposure media and may be the result of particle adsorption on the root surface. We speculate that ^{13}C-nPS enters into roots *via* a crack-entry mode, as described by Li et al. (2020). ^{13}C-nPS might be transported to the stem tissue in some species (*B. pendula*) *via* the transpiration stream in the xylem. Although the ^{13}C enrichment in stems of *B. pendula* was significant and an overall treatment effect on leaves was observed, ^{13}C enrichment remained low, which can most likely be attributed to dilution in the large stem biomass. Future experiments with different exposure times, higher concentrations of ^{13}C-nPS, or the use of more easily detected isotopes (*e.g.*, ^{14}C) would help to identify the magnitude of within-tree transport of nanoplastics. As indicated by this study, the uptake of nanoplastics by trees may affect tree physiological functions and allow nanoplastics to enter the food chain in forest ecosystems, as has been observed in marine environments.

Acknowledgements

We would like to express our thanks to Brian Sinnet (EAWAG) for his advice and help running the DLS analyses and to our colleagues at the WSL Claudio Cattaneo and Gabor Reiss for helping in the greenhouse; Dr. Jobin Joseph, Dr. Leonie Schönbeck, Shengnan Ouyang, and Dr. Marco Pecchia for helping to set up the experiment and collect data; Liska Dällenbach, Luc Schnell, Nadja-Tamara Studer, and Dr. Nasrullah Khan for helping with the harvest; and Manuela Oettli for running the isotope-ratio mass-spectrometer analysis. We would like to thank Ms. Erin Gleeson of SciencEdit.CH for her help revising a previous draft of this paper. We acknowledge financial support from the Swiss Federal Research Institute WSL.

Authors' contributions

Conceptualization: MEM, PC, AG, IB, FH; Methodology: MEM, PC, AG, IB, FH, RG, MASC; Collection of data: MEM, PC, AG, PB; Data analysis: MEM, AG, MS, FH; Writing-original draft preparation: MEM, PC, AG, IB, FH; Writing-review and editing: MEM, AG, PC, IB, RG, MS, PB, FH, MASC, GO; Funding acquisition: PC, AG; Supervision: PC, AG, IB, FH.

References

Allen S, Allen D, Phoenix VR, Le Roux G, Durantez Jimenez P, Simonneau A, Binet S, Galop D (2019). Atmospheric transport and deposition of microplastics in a remote mountain catchment. Nature Geoscience 12: 339-344. - doi: 10.1038/s41561-019-0335-5

Al-Sid-Cheikh M, Rowland SJ, Kaegi R, Henry TB, Cormier MA, Thompson RC (2020). Synthesis of 14C-labelled polystyrene nanoplastics for environmental studies. Communications Materials 1: 1-8. - doi: 10.1038/s43246-020-00097-9

Ambrosini R, Azzoni RS, Pittino F, Diolaiuti G, Franzetti A, Parolini M (2019). First evidence of microplastic contamination in the supraglacial debris of an alpine glacier. Environmental pollution 253: 297-301. - doi: 10.1016/j.envpol.2019.07.005

Azeem I, Adeel M, Ahmad MA, Shakoor N, Jiangcuo GD, Azeem K, Ishfaq M, Shakoor A, Ayaz M, Xu M, Rui Y (2021). Uptake and accumulation of nano/microplastics in plants: a critical review. Nanomaterials 11 (11): 2935. - doi: 10.3390/nano11112935

Bergmann M, Mützel S, Primpke S, Tekman MB, Trachsel J, Gerdts G (2019). White and wonderful? Microplastics prevail in snow from the Alps to the Arctic. Science Advances 5: eaax1157. - doi: 10.1126/sciadv.aax1157

Bosker T, Bouwman LJ, Brun NR, Behrens P, Vijver MG (2019). Microplastics accumulate on pores in seed capsule and delay germination and root growth of the terrestrial vascular plant *Lepidium sativum*. Chemosphere 226: 774-781. - doi: 10.1016/j.chemosphere.2019.03.163

Brahney J, Hallerud M, Heim E, Hahnenberger M, Sukumaran S (2020). Plastic rain in protected areas of the United States. Science 368: 1257-1260. - doi: 10.1126/science.aaz5819

Brahney J, Mahowald N, Prank M, Cornwell G, Klimont Z, Matsui H, Prather KA (2021). Constraining the atmospheric limb of the plastic cycle. Proceedings of the National Academy of Sciences USA 118: e2020719118. - doi: 10.1073/pnas.2020719118

Choi YR, Kim YN, Yoon JH, Dickinson N, Kim KH (2020). Plastic contamination of forest, urban, and agricultural soils: a case study of Yeoju City in the Republic of Korea. Journal of Soils and Sediments 21: 1962-1973. - doi: 10.1007/s11368-020-02759-0

De Souza Machado AA, Kloas W, Zarfl C, Hempel S, Rillig MC (2018). Microplastics as an emerging threat to terrestrial ecosystems. Global Change Biology 24: 1405-1416. - doi: 10.1111/gcb.14020

De Souza Machado AA, Lau CW, Kloas W, Bergmann J, Bachelier JB, Faltin E, Becker R, Görlich A, Rillig MC (2019). Microplastics can change soil properties and affect plant performance. Environmental Science Technology 53: 6044-6052. - doi: 10.1021/acs.est.9b01339

Dovidat LC, Brinkmann BW, Vijver MG, Bosker T (2020). Plastic particles adsorb to the roots of freshwater vascular plant *Spirodela polyrhiza* but do not impair growth. Limnology and Oceanography Letters 5: 37-45. - doi: 10.1002/lol2.10118

Dris R, Gasperi J, Saad M, Mirande C, Tassin B (2016). Synthetic fibers in atmospheric fallout: a source of microplastics in the environment? Marine Pollution Bulletin 104: 290-293. - doi: 10.1016/j.marpolbul.2016.01.006

Gasperi J, Wright SL, Dris R, Collard F, Mandin C, Guerrouache M, Langlois V, Kelly FJ, Tassin B (2018). Microplastics in air: are we breathing it in? Current opinions in Environmental Science and Health 1: 1-5. - doi: 10.1016/j.coesh.2017.10.002

Gessler A, Kreuzwieser J, Dopatka T, Rennenberg H (2002). Diurnal courses of ammonium net uptake by the roots of adult beech (*Fagus sylvatica*) and spruce (*Picea abies*) trees. Plant and Soil 240: 23-32. - doi: 10.1023/A:1015831304911

Geyer R, Jambeck JR, Law KL (2017). Production, use, and fate of all plastics ever made. Science Advances 3 (7): 615. - doi: 10.1126/sciadv.1700782

Giorgetti L, Spanò C, Muccifora S, Bottega S, Barbieri F, Bellani L, Ruffini Castiglione M (2020). Exploring the interaction between polystyrene nanoplastics and *Allium cepa* during germination: Internalization in root cells, induction of toxicity and oxidative stress. Plant Physiology and Biochemistry 149: 170-177. - doi: 10.1016/j.plaphy.2020.02.014

Huerta Lwanga E, Gertsen H, Gooren H, Peters P, Salánki T, Van Der Ploeg M, Besseling E, Koelmans AA, Geissen V (2016). Microplastics in the terrestrial ecosystem: implications for *Lumbricus terrestris* (Oligochaeta, Lumbricidae). Environmental Science and Technology 50: 2685-2691. - doi: 10.1021/acs.est.5b05478

Jambeck JR, Geyer R, Wilcox C, Siegler TR, Perryman M, Andrady A, Narayan R, Law KL (2015). Plastic waste inputs from land into the ocean. Science 347: 768-771. - doi: 10.1126/science.1260352

Lehner R, Weder C, Petri-Fink A, Rothen-Rutishauser B (2019). Emergence of nanoplastic in the environment and possible impact on human health. Environmental Science and Technology 53: 1748-1765. - doi: 10.1021/acs.est.8b05512

Leuschner C (2002). Forest succession and water resources: soil hydrology and ecosystem water turnover in early, mid and late stages of a 300-yr-long chronosequence on sandy soil. In: "Forest Development: Succession, Environmental Stress and Forest Management" (Dohrenbusch A, Bartsch N eds). Springer, Berlin, Heidelberg, Germany, pp. 1-68. - doi: 10.1007/978-3-642-55663-0_1

Li L, Luo Y, Li R, Zhou Q, Peijnenburg WJ, Yin N, Yang J, Tu C, Zhang Y (2020). Effective uptake of submicrometre plastics by crop plants via a crack-entry mode. Nature Sustainability 3: 929-937. - doi: 10.1038/s41893-020-0567-9

Liu Y, Guo R, Zhang S, Sun Y, Wang F (2022). Uptake and translocation of nano/microplastics by rice seedlings: evidence from a hydroponic experiment. Journal of Hazardous Materials 421: 126700. - doi: 10.1016/j.jhazmat.2021.126700

Lozano YM, Lehnert T, Linck LT, Lehmann A, Rillig MC (2021a). Microplastic shape, concentration and polymer type affect soil properties and plant biomass. Frontiers in Plant Science 12: 339. - doi: 10.3389/fpls.2021.616645

Lozano YM, Aguilar-Trigueros CA, Onandia G, Maa S, Zhao T, Rillig MC (2021b). Effects of microplastics and drought on soil ecosystem functions and multifunctionality. Journal of Applied Ecology 58: 988-996. - doi: 10.1111/1365-2664.13839

Materić D, Ludewig E, Brunner D, Röckmann T, Holzinger R (2021). Nanoplastics transport to the remote, high-altitude Alps. Environmental Pollution 288: 117697. - doi: 10.1016/j.envpol.2021.117697

Mitrano DM, Wohlleben W (2020). Microplastic regulation should be more precise to incentivize both innovation and environmental safety. Nature Communications 11: 1-12. - doi: 10.1038/s41467-020-19069-1

Patil SM, Rane NR, Bankole PO, Krishnaiah P, Ahn Y, Park YK, Yadav KK, Amin MA, Jeon BH (2022). An assessment of micro-and nanoplastics in the biosphere: a review of detection, monitoring, and remediation technology. Chemical Engineering Journal 430 (7): 132913. - doi: 10.1016/j.cej.2021.132913

Rezaei M, Riksen MJPM, Sirjani E, Sameni A, Geissen V (2019). Wind erosion as a driver for transport of light density microplastics. Science of the Total Environment 669: 273-281. - doi: 10.1016/j.scitotenv.2019.02.382

Rillig MC, Ingraffia R, De Souza Machado AA (2017). Microplastic incorporation into soil in agroecosystems. Frontiers in Plant Science 8: 249. - doi: 10.3389/fpls.2017.01805

Ruehr NK, Offermann CA, Gessler A, Winkler JB, Ferrio JP, Buchmann N, Barnard RL (2009). Drought effects on allocation of recent carbon: from beech leaves to soil CO_2 efflux. New Phytologist 184: 950-961. - doi: 10.1111/j.1469-8137.2009.03044.x

Scheurer M, Bigalke M (2018). Microplastics in Swiss floodplain soils. Environmental Science Technology 52: 3591-3598. - doi: 10.1021/acs.est.7b06003

Sun X-D, Yuan X-Z, Jia Y, Feng L-J, Zhu F-P, Dong S-S, Liu J, Kong X, Tian H, Duan J-L, Ding Z, Wang S-G, Xing B (2020). Differentially charged nanoplastics demonstrate distinct accumulation in *Arabidopsis thaliana*. Nature Nanotechnology 15: 755-760. - doi: 10.1038/s41565-020-0707-4

Van Weert S, Redondo-Hasselerharm PE, Diepens NJ, Koelmans AA (2019). Effects of nanoplastics and microplastics on the growth of sediment-rooted macrophytes. Science of the Total Environment 654: 1040-1047. - doi: 10.1016/j.scitotenv.2018.11.183

Wagner S, Reemtsma T (2019). Things we know and don't know about nanoplastic in the environment. Nature Nanotechnology 14: 300-301. - doi: 10.1038/s41565-019-0424-z

Wang F, Wang Q, Adams CA, Sun Y, Zhang S (2022). Effects of microplastics on soil properties: current knowledge and future perspectives. Journal of Hazardous Materials 424 (21): 127531. - doi: 10.1016/j.jhazmat.2021.127531

Windsor FM, Durance I, Horton AA, Thompson RC, Tyler CR, Ormerod SJ (2019). A catchment-scale perspective of plastic pollution. Global Change Biology 25: 1207-1221. - doi: 10.1111/gcb.14572

Zhang T, Wang C, Dong F, Gao Z, Zhang C, Zhang X, Fu L, Wang Y, Zhang J (2019). Uptake and translocation of styrene maleic anhydride nanoparticles in *Murraya exotica* plants as revealed by noninvasive, real-time optical bioimaging. Environmental Science and Technology 53: 1471-1481. - doi: 10.1021/acs.est.8b05689

Supplementary Material

Fig. S1 - Secondary electron (SE) images.

Tab. S1 - Detailed data on dry weight, $\delta^{13}C$, atom % and the amount of ^{13}C (g) in each tissue of each replicate plant.

Link: Murazzi_4021@suppl001.pdf

Tree Physiology 39, 1251–1261
doi:10.1093/treephys/tpz046

Research paper

Silver nanoparticles enter the tree stem faster through leaves than through roots

C. Cocozza[1,10], A. Perone[2], C. Giordano[3], M. C. Salvatici[4], S. Pignattelli[5], A. Raio[5], M. Schaub[6], K. Sever[7], J.L. Innes[8], R. Tognetti[9] and P. Cherubini[6,8]

[1]Dipartimento di Scienze e Tecnologie Agrarie, Alimentari, Ambientali e Forestali, Università di Firenze, via San Bonaventura 13, 50145 Florence, Italy; [2]Dipartimento di Bioscienze e Territorio, Università degli Studi del Molise, c.da Fonte Lappone snc, 86090 Pesche, Italy; [3]Istituto Valorizzazione Legno e Specie Arboree, IVALSA-CNR, via Madonna del Piano 10, 50019 Firenze, Italy; [4]Istituto di Chimica dei Composti Organo Metallici, ICCOM-CNR, via Madonna del Piano 10, 50019 Firenze, Italy; [5]Istituto per la Protezione Sostenibile delle Piante, IPSP-CNR, via Madonna del Piano 10, 50019 Sesto Fiorentino, Italy; [6]WSL, Swiss Federal Institute for Forest, Snow and Landscape Research, Zürcherstrasse 111, 8903 Birmensdorf, Switzerland; [7]Department of Forest Genetics, Dendrology and Botany, Faculty of Forestry, University of Zagreb, Svetošimunska cesta 25, 10000 Zagreb, Croatia; [8]Faculty of Forestry, University of British Columbia, 2424 Main Mall, BC V6T 1Z4, Vancouver, Canada; [9]Dipartimento di Agricoltura, Ambiente e Alimenti, Università degli Studi del Molise, via de Sanctis sns, 86100 Campobasso, Italy; [10]Corresponding author (claudia.cocozza@unifi.it)

Received August 26, 2018; accepted April 6, 2019; handling Editor Kathy Steppe

A major environmental pollution problem is the release into the atmosphere of particulate matter, including nanoparticles (NPs), which causes serious hazards to human and ecosystem health, particularly in urban areas. However, knowledge about the uptake, translocation and accumulation of NPs in plant tissues is almost completely lacking. The uptake of silver nanoparticles (Ag-NPs) and their transport and accumulation in the leaves, stems and roots of three different tree species, downy oak (*Quercus pubescens* Willd.), Scots pine (*Pinus sylvestris* L.) and black poplar (*Populus nigra* L.), were assessed. In the experiment, Ag-NPs were supplied separately to the leaves (via spraying, the foliar treatment) and roots (via watering, the root treatment) of the three species. Uptake, transport and accumulation of Ag were investigated through spectroscopy. The concentration of Ag in the stem was higher in the foliar than in the root treatment, and in poplar more than in oak and pine. Foliar treatment with Ag-NPs reduced aboveground biomass and stem length in poplars, but not in oaks or pines. Species-specific signals of oxidative stress were observed; foliar treatment of oak caused the accumulation of H_2O_2 in leaves, and both foliar and root treatments of poplar led to increased O_2^- in leaves. Ag-NPs affected leaf and root bacteria and fungi; in the case of leaves, foliar treatment reduced bacterial populations in oak and poplar and fungi populations in pine, and in the case of roots, root treatment reduced bacteria and increased fungi in poplar. Species-specific mechanisms of interaction, transport, allocation and storage of NPs in trees were found. We demonstrated definitively that NPs enter into the tree stem through leaves faster than through roots in all of the investigated tree species.

Keywords: Ag-NPs, pathway of uptake, *Pinus sylvestris* L., *Populus nigra* L., *Quercus pubescens* Willd.

Introduction

The release of particulate matter (PM_{10} and $PM_{2.5}$, particles with diameters 10 and 2.5 μm and smaller, and nanoparticles (NPs), i.e., having at least one dimension smaller than 100 nm) from natural and anthropogenic sources into the environment causes significant hazards to human, animal and plant health and life, particularly in urban areas (Dietz and Herth 2011, Tripathi et al. 2017). Because of their accumulation, exposure concentrations are predicted to be higher in soils than in the atmosphere. Although accumulation of NPs by plants is generally proportional to exposure concentration, the specific

relevance of various leaf and root structures (e.g., leaf stomata, leaf cuticle and root hairs and Casparian band) in plant uptake remains unclear. Tree species, wood anatomy, soil chemistry, climatic conditions and particle characteristics have all been reported to play a role in metal uptake, mobilization, translocation and storage processes (Cutter and Guyette 1993). Plants can absorb and translocate NPs through the root tissues (Wang et al. 2016). After adsorption on the root surface, pollutants penetrate the roots passively and are translocated via the water system (Shahid et al. 2014). Plant canopies also play an important role in the capture of airborne NPs (Birbaum et al. 2010, Nair et al. 2010, Larue et al. 2014, Sgrigna et al. 2015). Foliar uptake of NPs is affected by several factors, including size and form of NPs (e.g., Raliya et al. 2016), environmental conditions (e.g., Wang et al. 2013), plant species (Birbaum et al. 2010, Wang et al. 2013) and mode of application (e.g., Hong et al. 2014). Pollutants can be bound to the leaf surface through cuticular wax, as well as diffuse through the lipophilic elements of cuticle and leaf hairs (Li et al. 2017) and via aqueous pores of stomata (Larue et al. 2014). Once inside the cells, NPs can be transported apoplastically or symplastically through plasmodesmata (Rico et al. 2011), with detrimental effects on plant productivity (Nel et al. 2006). We speculate that NPs enter into the stem wood through the leaves at different rates in comparison with the roots, depending on organ-specific physiological and biochemical processes and morphological and structural barriers, in addition to the size of NPs. Here, we present an experiment designed to clarify the uptake of NPs through the leaves and roots and their translocation and storage into tree stems. Recent progress in analytical techniques enables the detection of very low concentrations of pollutants in wood that may become a reliable indicator of changes in environmental chemical conditions.

In this study, silver nanoparticles (Ag-NPs) were selected due to their designation as an Organization for Economic Co-operation and Development priority nanomaterial (OECD 2010). In nature, Ag occurs in basalt (0.1 mg kg^{-1}) and igneous rocks (0.07 mg kg^{-1}) and tends to be concentrated in crude oil and in water from hot springs and steam wells (Howe and Dobson 2002). Anthropogenic sources of Ag include smelting, hazardous waste sites, cloud seeding with Ag iodide, metal mining, sewage outfalls and the photo processing industry (Eisler 1997). Applications of Ag are common in medicine, cosmetics, sporting equipment, environmental remediation and information technology (Maillard and Hartemann 2012). Yin et al. (2012) reported higher Ag content in Italian ryegrass with increasing concentration of Ag-NPs. Yet, Ag-NPs are used as an efficient fungicide (Kim et al. 2013) and inhibit the growth of Gram-positive and Gram-negative bacteria (Samberg et al. 2011). Seed germination of cucumber and lettuce seeds (Barrena et al. 2009) and ryegrass and barley (El-Temsah and Joner 2012) was reduced by exposure to Ag-NPs (size 29 and 1–20 nm, respectively). Although Ag-NPs damage plant functionality and, consequently, plant growth (Lee et al. 2008, Yin et al. 2012), the mechanisms of uptake, translocation, storage and toxicity of Ag-NPs remain largely unknown. In plants, the impact of Ag-NPs can be related to the overproduction of reactive oxygen species (ROS), inducing oxidative stress with consequent damage to proteins, lipids and carbohydrates and to carbon assimilation and biomass production (Yin et al. 2012, Dimkpa et al. 2013).

While NPs may accumulate in woody tissues once transported through the vascular system (Seeger et al. 2009, Schreck et al. 2014, Shahid et al. 2017), the role of foliar and root uptake in element speciation, toxicity, compartmentalization and detoxification in trees has rarely been explored (Smita et al. 2012, Schwab et al. 2016). Most studies of NP accumulation have been carried out on crops (e.g., Yang et al. 2006, Lin and Xing 2007); few such studies exist for trees (but see, e.g., Nowack and Bucheli 2007, Navarro et al. 2008, Zhai et al. 2014, Olchowik et al. 2017).

The goals of our experiment were to determine (i) if trees take up Ag-NPs, (ii) if Ag-NPs enter mainly through the roots or through the leaves and (iii) if Ag-NPs enter into the wood cells faster through the roots or through the leaves. Ag-NPs were supplied separately to the leaves (by spraying) and roots (by watering) of three woody species: downy oak, black poplar and Scots pine. Ag-NPs were localized and quantified within above- and belowground plant organs, and their effects on plant growth and function were assessed. We tested whether the impact of Ag-NPs on the three forest trees after foliage and soil application results in differential changes in the accumulation of Ag, the photosynthetic response curves to CO_2, the induction of oxidative stress, the biomass of tree seedlings and the development of the microbiome, depending on the species of tree and/or type of supply.

Materials and methods

Plant material and experimental set-up

Ag-NPs were supplied separately to the leaves and roots of potted *Quercus pubescens* Willd. (downy oak), *Populus nigra* L. (black poplar) and *Pinus sylvestris* L. (Scots pine) under controlled conditions in a greenhouse. Ag-NPs nanoparticles (coated with amorphous carbon) were obtained from Novacentrix Corporation (Austin, TX, USA) and used for the experiment. The Ag-NPs were 98% pure, had average diameters of between 10 and 40 nm and a specific surface area of 23 m^2 g^{-1}. A 10 l solution was created by directly dispersing the Ag-NPs in water and adding a few drops of a surfactant substance (commercial dish soap) to reduce the surface tension of the water.

In winter 2015, 40 3-year-old trees of each species were planted into individual 15 l plastic pots filled with a soil–fertilizer mixture. Trees were grown in a greenhouse under well-watered conditions, defined by a complete replenishment of the amount of water lost each week as assessed by measuring the change in weight of each pot as described by Regier et al. (2009). After 4 months of growth, in May 2016, 24 trees of each species of similar height were selected and trimmed to a single shoot. Temperature and humidity were kept constant (20 °C at night and 25 °C during the day with 40–60% relative humidity). The experimental layout was a randomized block design with eight replicates (trees) for the three species (oak, poplar, pine) and three treatments: 'control', trees were pot-watered with tap water; 'root treatment', trees were pot-watered with 400 ml Ag-NPs solution (corresponding to the weekly evapotranspirated water); and 'foliar treatment', trees were treated with Ag-NPs on both sides of the foliage by spraying with 200 ml of solution (the amount of water retained by the foliage). The foliar treatment was performed in a separate greenhouse room to avoid contamination, while covering the top of the pot with a plastic membrane to avoid contamination of the soil. Ag-NPs were supplied weekly in a solution with a concentration of 1 mg Ag-NPs l^{-1} of water. This concentration was chosen according to Wang et al. (2013). No fertilizer was used during the experiment. Treatments were performed over 10 weeks from 19 May to 28 July 2016 (4 weeks with a single weekly supply, followed by 6 weeks with a twice weekly supply), simulating a chronic exposure to NPs.

Determination of Ag

ICP-MS Roots, leaves, stems and bulk soils ($n = 5$) were sampled at the end of the experiment and dried at 80 °C until they reached constant weight, then ground in a metal-free mill (Retsch GmbH, Haan, Germany). Leaf tissues of foliar treatment trees were washed in distilled water according to Ugolini et al. (2013) to enable the detection of Ag adsorbed on the tissue surface versus that absorbed in the tissue. To determine the concentration of NPs, 0.5 g of roots, leaves, stems and soil samples was digested in aqua regia (nitric acid:hydrochloric acid, 3:1). Digested samples were diluted with 4.5 ml 1% nitric acid. The concentration of Ag (µg kg^{-1}) in each sample was measured using inductively coupled plasma mass spectrometry (ICP-MS; PerkinElmer, Waltham Massachusetts, USA), a method for analysis of target elemental species (Feldmann et al. 2018).

ESEM Leaves were analyzed using an FEI Quanta 200 environment scanning electron microscope (ESEM; FEI Corporation, Eindhoven, The Netherlands), operating in low vacuum mode (the chamber pressure was kept at 130 Pa) at 25 kV, without preparation of the samples. The ESEM images (300× magnification) of upper and lower leaf surfaces were analyzed using the ImageJ analysis software. Stomatal size and density (number mm^{-2}), trichrome typology, density and length per unit area (mm^{-2}) were measured on control and treated leaves that were formed under the experimental conditions.

Plant traits analysis

Plant growth Stem and root lengths were measured at the end of the experiment. Biomass allocation in the different organs (roots, leaves and stems) of control, foliage- and root-treated trees were determined as dry weight (DW) after 24 h of drying in an oven at 80 °C. The ratio between the biomass of non-photosynthetic and photosynthetic organs ('C/F') was calculated by dividing the sum of stem and root and leaf DW (Monsi and Saeki 2005).

Photosynthetic response curves Photosynthetic response curves (A/Ci curves), derived from the response of net photosynthesis (A) to intercellular CO_2 concentration (C_i), were measured on the third fully expanded mature leaf, formed during the experiment, from the stem apex in oak and poplar and on the branch of the first whorl in pine. Measurements were conducted with three trees from each species–treatment combination after 4 weeks of single Ag-NPs treatment (13 June) using a portable photosynthesis system (Li-Cor 6,400, Lincoln, NE, USA). The measurement was repeated at the end of the treatment (28 July). The leaf was clamped in a 6 cm^2 Li-Cor 6400 cuvette. The CO_2 response curves were obtained by changing the [CO_2] entering the cuvette from 50 to 800 µmol mol^{-1} with an external CO_2 cartridge mounted on the Li-Cor 6400 console and automatically controlled by a CO_2 injector. The CO_2 assimilation rate was first measured by setting the reference [CO_2] near ambient (400 µmol mol^{-1}) and then at 300, 200, 100, 50, 400, 600 and 800 µmol mol^{-1}. Gas exchange was determined at each step after exposure of the leaf to the new [CO_2] for 60–120 s; photosynthetic active radiation was maintained at 1500 µmol m^{-2} s^{-1}, 28 °C block temperature and a relative humidity of 60%.

The maximum rate of ribulose-1,5-bisphosphate carboxylation (Vc_{max}), the maximum rate of electron transport used in the regeneration of RuBP (J_{max}), triose phosphate use (TPU), mesophyll conductance (g_m) and day respiration (R_{day}) were computed from the A/Ci curves using the A/Ci curve-fitting model developed by Sharkey et al. (2008). Triose phosphate use was determined as the highest A, regardless of whether symptoms of TPU were present, which makes TPU similar to the parameter A_{max} reported by other investigators. Gas exchange in Scots pine is reported on a unit surface area basis calculated using a geometric approximation of the needle surface.

Determination of ROS and antioxidant compounds Hydrogen peroxide (H_2O_2) was measured spectrophotometrically after reaction with KI, according to a method proposed by

Alexieva et al. (2001). The reaction was developed in trichloroacetic acid (TCA) and absorbance measured at 390 nm. The amount of H_2O_2 was calculated using a standard curve prepared with known concentrations of H_2O_2. The results were expressed as μg g^{-1} leaf fresh weight.

Superoxide anion (O_2^-) was measured as described by Elstner and Heupel (1976) by monitoring the nitrite formation from hydroxylamine in the presence of O_2^-, with some modifications (Jiang and Zhang 2001). The sample was read at 530 nm. A calibration curve was established using sodium nitrite. The results were expressed as μg g^{-1} leaf fresh weight.

Ascorbic acid (AsA) concentration was determined through the method proposed by Okamura (1980) and modified by Law et al. (1983). The assay was based on the reduction of Fe^{3+} to Fe^{2+} by ascorbate (As) in acidic solution. The absorbance at 525 nm was recorded. A standard curve of ascorbic acid (AsA) was used for calibration. The results were expressed as μg g^{-1} fresh leaf weight.

Glutathione (GSH) was determined using a modification of the Sedlak and Lindsay (1968) method. The determination was obtained through the reaction in TCA and the absorbance was read at 412 nm. A standard curve of GSH was used for calibration. The results were expressed as μg g^{-1} fresh leaf weight.

Determination of cultivable bacteria and fungi

Cultivable bacteria and fungi concentrations in leaves and roots were determined for three trees per species. Leaves and roots were randomly collected from three trees of each treatment. Before the suspension preparation, roots were vigorously shaken to eliminate the coarse soil particles. Five grams of leaves and capillary roots were suspended in 90 ml of saline buffer (0.8% NaCl) and shaken for 1 h at room temperature. Suspensions were serially diluted and aliquots of 100 μl of each dilution were spread on agar media specific for the two different microbial groups: tryptic soy agar medium amended with 200 ppm cycloheximide for bacteria isolation and potato dextrose agar acidified with a solution of 25% lactic acid (200 μl l^{-1}) and amended with 100 ppm streptomycin for fungi isolation (Schaad et al. 2001). Plates were incubated at 27 °C and monitored for 1 week. Colonies were counted and the number of colony forming units (cfu) per gram of leaves or roots was calculated (cfu g^{-1}).

Statistical analysis

All data were presented as mean ± standard error (SE) based on at least five replicates per treatment. Data were analyzed using one-way analysis of variance (ANOVA) to assess the difference between treatments for the measured parameters. A post hoc comparison of means was performed using the least significant difference (Tukey-HSD) test at the 0.05 significance level. Statistical analyses were performed with the OriginPro9.1 (OriginLab, Northampton, Massachusetts, USA) scientific data analysis and graphing software.

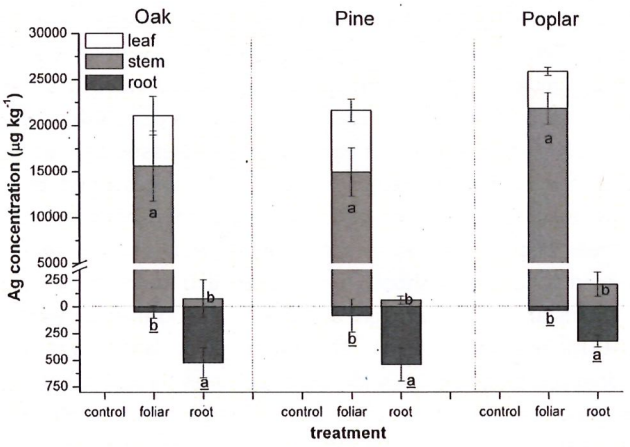

Figure 1. Silver concentration (μg kg^{-1}) in root, stem and leaf of oak, pine and poplar plants supplied with Ag-NPs for 10 weeks. Data refer to control, foliar and root treatments with Ag-NPs. The values are the mean ± SD (n = 5). Different letters correspond to statistical differences between treatments within tissues (lowercase letters for stem; underlined letters for root) (Tukey-HSD, $P < 0.05$ level).

Results

Silver in trees

The concentration of Ag (μg kg^{-1}; Figure 1) varied among plant tissues (root, stem and leaf) and treatments ('control', 'foliar' and 'root') within each species. In foliar treatment trees, Ag concentrations (μg kg^{-1}) were higher in leaves and stems than in roots. Poplar foliar treatment trees showed the highest Ag concentration in the stem, with 21,808.99 (±1714.72) μg kg^{-1}, which represents 84.3% of the total Ag concentration detected; concentrations were lower in leaves (15.5%) and roots (0.1%). A similar trend across organs was found in the other two species: pine showed Ag concentrations of 73.8%, 25.8% and 0.23%, whereas oak showed Ag concentrations of 68.7%, 30.8% and 0.4%, in stem, leaves and roots, respectively. Silver was not found in the leaves of any root treatment trees, regardless of species (Figure 1). The concentration of Ag in soil samples of root treatment trees was 7.47 ± 0.1 μg kg^{-1}, 25.0 ± 0.3 μg kg^{-1} and 12.99 ± 0.2 μg kg^{-1} in oak, pine and poplar, respectively; in foliar treatment trees, it was 2.88 ± 0.1 μg kg^{-1}, 7.24 ± 0.2 μg kg^{-1} and 1.01 ± 0.1 μg kg^{-1} in oak, pine and poplar, respectively.

Effects on plant growth

Biometric traits in poplar showed significant differences between treatments ($P < 0.05$) (Figure 2). In foliar treatment trees,

Table 1. Ratio of DW ('C/F') of non-photosynthetic (the sum of stem and root tissues) and photosynthetic organs (leaf tissues) in oak, pine and poplar plants exposed to control, foliar and root treatments. The values are the mean ± SD ($n = 5$). One-way ANOVA was applied to determine significant differences between treatments within each species (P value is given; ns, not significant).

Species	Treatment	C/F (g g^{-1})	P-level
Oak	Control	1.40 ± 0.08	ns
	Foliar	1.50 ± 0.05	
	Root	1.36 ± 0.07	
Pine	Control	3.07 ± 0.08	ns
	Foliar	3.65 ± 0.05	
	Root	2.96 ± 0.07	
Poplar	Control	2.24 ± 0.41	0.05
	Foliar	1.66 ± 0.14	
	Root	1.32 ± 0.05	

poplar showed a significant reduction in biomass of leaf and stem tissues, as well as in stem length and 'C/F'. In contrast, no significant differences between treatments were found in oak or pine (Figure 2 and Table 1).

Photosynthetic capacity parameters (Vc_{max}, TPU, R_{day}) and internal CO_2 diffusion (g_m) did not change between treatments. The J_{max} varied significantly among the three species, being higher in foliar treatment poplars (13 June), lower in root treatment pines (13 June) and oaks (18 July), and lower in foliar treatment pines (18 July). The Vc_{max} was significantly lower in foliar treatment (13 June) poplars than in the other two species (Table 2).

Significant differences in stomatal density between treatments were observed in poplar but not in oak or pine (Figure 3A). Stomatal density differed between treatments on the abaxial leaf surface of poplar, showing higher values in foliar treatment trees (205.2 ± 17.1 stomata mm^{-2}) than in root treatment and control trees. No treatment-related differences in stomatal density were found on the adaxial leaf surface (Figure 3A).

Stomatal length differed between treatments in the three species (Figure 3B), being longer in foliar treatment and root treatment oaks and pines in comparison with control trees, but longer in control poplars (Figure 3B). In poplar, stomatal length was significantly different between treatments on both the abaxial and adaxial leaf surfaces (Figure 3B).

The trichome structure in leaves of oak was affected by the treatment (Figure 3C). Trichome density was significantly lower on the abaxial and adaxial leaf surfaces of foliar treatment trees than control trees. It was significantly lower on the adaxial leaf surface of control and foliar treatment trees than on the adaxial leaf surfaces of root treatment trees. Trichome length was significantly different between foliar treatment trees as compared with trees with other treatments (Figure 3C).

The ROS showed a significant accumulation of H_2O_2 in foliar treatment oak trees. In poplar, higher values of O_2^- were found in leaves of foliar treatment and root treatment trees in comparison with control trees. Reactive oxygen species contents were not detected in pine (Figure 4).

The concentration of antioxidant compounds (AOX) showed that AsA was significantly higher in root treatment pine and poplar trees in comparison with control trees (Figure 4). In pine and poplar, GSH concentration was higher in root treatment trees than in foliar treatment and control trees of pine; GSH was not significantly different between treatments in oak and poplar (Figure 4).

Bacterial and fungal populations of leaves and roots in foliar treatment and root treatment trees were affected by Ag-NPs treatment, respectively; root treatment did not affect epiphytic populations and foliar treatment did not affect root populations. Foliar treatment trees showed significantly smaller epiphytic bacterial populations in oak and poplar and smaller fungal populations in pine (Table 3). The root treatment did not affect microbial populations in oak and pine roots, but bacteria were significantly reduced in poplar roots. In contrast, an increase in the concentration of root fungi was detected in poplar following Ag-NPs root treatment (Table 3).

Discussion

Silver in plant tissues

Oak, pine and poplar concentrated Ag-NP in aboveground tissues, with more than 50% of the total Ag in the stem when exposed to foliar treatment, though with differences among species. In contrast, root treatment trees had no Ag in their leaves and the Ag concentrations in their stems were lower than in foliar treatment trees. The Ag concentration was lower in poplar leaves than in oak and pine leaves (15.5%, 25.8% and 30.8% of the Ag in the plant was in the leaf of poplar, oak and pine, respectively; Figure 1), possibly due to the high carboxylation rate of poplar, corresponding to high photosynthesis rate. This might favor stem wood production and transport to the phloem (Kim et al. 2008) in comparison with the other two species. The absorption, accumulation and translocation of NPs in trees depends strictly on the properties of the NPs, though species-specific structural and functional traits of plant organs (leaves, roots and stems) and their biomass play an important role (Ma et al. 2010, Shahid et al. 2017). Differences in Ag concentrations across above- and belowground organs and among species indicate complex uptake, transport and accumulation processes.

Stomatal length ranged between 15 and 40 µm, which makes stomata a potential route for uptake of Ag-NPs (mean diameter 25 nm), applied in dispersed form on the leaf surface, probably diffused in dispersed form through a water film. Foliar uptake of NPs is driven by stomatal penetration (Eichert et al. 2008), and the stomatal pathway is favored by high air humidity, such as a droplet covering the stomata and the condensation of

Table 2. Maximum carboxylation rate (Vc_{max}), electron transport rate (J_{max}), TPU, day respiration (R_{day}) and mesophyll conductance (g_m) in oak, pine and poplar plants supplied with Ag-NPs for 10 weeks. The values are the mean ± SD ($n = 5$). One-way ANOVA was applied to determine significant differences between treatments within each species (P-level is given; ***, $P < 0.001$; ns, not significant).

	Species	Treatment	Vc_{max} ($\mu mol\ m^{-2}\ s^{-1}$) Mean SE	J_{max} ($\mu mol\ m^{-2}\ s^{-1}$) Mean SE	TPU ($\mu mol\ m^{-2}\ s^{-1}$) Mean SE	R_{day} ($\mu mol\ m^{-2}\ s^{-1}$) Mean SE	Gm ($mmol\ m^{-2}\ s^{-1}$) Mean SE
13 June	Oak	Control	35.4 ± 2.9	411.1 ± 18.0	6.1 ± 0.6	1.6 ± 0.2	25.4 ± 0.6
		Foliar	34.7 ± 0.9	430.9 ± 2.0	6.5 ± 0.3	2.6 ± 1.6	23.4 ± 2.5
		Root	37.8 ± 1.9	430.9 ± 0.1	7.0 ± 0.3	2.2 ± 1.0	26.2 ± 0.6
			ns	ns	ns	ns	ns
	Pine	Control	21.2 ± 1.9	406.4 ± 19.8	5.7 ± 0.9	2.3 ± 0.5	26.2 ± 0.2
		Foliar	24.2 ± 1.9	401.3 ± 30.0	5.8 ± 0.8	1.6 ± 0.2	26.4 ± 0.3
		Root	28.8 ± 1.5	69.7 ± 7.1	6.6 ± 0.5	1.6 ± 0.1	26.2 ± 0.6
			ns	***	ns	ns	ns
	Poplar	Control	155.1 ± 6.8	83.4 ± 10.6	6.5 ± 0.9	2.3 ± 0.9	22.0 ± 2.5
		Foliar	38.5 ± 6.5	429.0 ± 0.9	5.9 ± 0.4	1.5 ± 0.2	26.5 ± 1.3
		Root	148.6 ± 13.1	84.9 ± 2.5	6.8 ± 0.4	2.0 ± 0.7	20.7 ± 3.0
			***	***	ns	ns	ns
18 July	Oak	Control	37.8 ± 9.4	428.0 ± 1.8	7.0 ± 1.2	1.6 ± 0.4	26.0 ± 0.9
		Foliar	29.5 ± 14.0	411.7 ± 15.1	4.3 ± 2.2	1.0 ± 0.7	27.6 ± 1.3
		Root	60.9 ± 5.8	298.2 ± 5.4	9.3 ± 0.7	1.9 ± 0.7	22.8 ± 4.1
			ns	***	ns	ns	ns
	Pine	Control	25.7 ± 12.7	412.9 ± 8.2	5.9 ± 1.8	4.8 ± 3.2	26.5 ± 1.7
		Foliar	36.1 ± 0.6	111.1 ± 48.7	7.4 ± 0.5	3.3 ± 2.1	25.8 ± 1.0
		Root	25.2 ± 16.9	412.9 ± 6.1	5.9 ± 2.1	3.0 ± 1.8	23.5 ± 3.8
			ns	***	ns	ns	ns
	Poplar	Control	75.0 ± 5.3	411.1 ± 29.1	7.2 ± 0.3	2.8 ± 1.0	24.6 ± 1.2
		Foliar	51.6 ± 1.4	433.2 ± 1.8	7.5 ± 0.7	3.0 ± 0.6	27.3 ± 0.8
		Root	42.8 ± 13.3	434.3 ± 1.9	7.1 ± 1.2	2.0 ± 0.6	27.1 ± 0.8
			ns	ns	ns	ns	ns

Table 3. Total fungal and bacterial population (cfu) in leaves and roots of oak, pine and poplar plants exposed to related Ag-NPs supply; leaf of foliar treatment and root of root treatments were considered. Data are reported in logarithmic scale. Significant differences between control and Ag-supply were reported (paired t-test): *$P < 0.05$; **$P < 0.01$; ***$P < 0.01$; ns, not significant.

Treatment	Tissue	Oak ($cfu\ g^{-1}$)		Pine ($cfu\ g^{-1}$)		Poplar ($cfu\ g^{-1}$)	
		Fungi	Bacteria	Fungi	Bacteria	Fungi	Bacteria
Control	Leaf	7.7×10^3	7.7×10^4	1.1×10^4	5.9×10^4	5.4×10^3	2.8×10^5
Foliar	Leaf	7.7×10^3	7.7×10^3	1.6×10^3	5.9×10^4	2.3×10^3	2.8×10^3
	P-level	ns	*	***	ns	ns	*
Control	Root	1.3×10^5	3.0×10^8	4.8×10^5	4.3×10^8	2.3×10^5	1.8×10^8
Root	Root	1.4×10^5	2.3×10^8	5.5×10^5	7.3×10^9	1.3×10^6	8.2×10^7
	P-level	ns	ns	ns	ns	**	*

water within the stomatal pores with the consequent uptake of particles (Eichert et al. 2008). The uptake of NPs may be limited by the closure of stomata at night or because of the reduced stomatal conductance under drought stress. However, several other species-specific resistances play an important role in the airborne NPs uptake, namely trichomes, stigma and hydathodes (Schwab et al. 2016, Wang et al. 2016). Despite a low cuticle thickness, poplar may retain high numbers of particles due to its large leaf surface area (Hull et al. 1975). Pine is characterized by hydrophobic epicuticular waxes (Percy et al. 2013), resulting in a low contact surface between cuticle and contaminants. Trichomes of oak leaves may trap NPs on the leaf surface, interfering with their translocation (Dietz and Herth 2011, Schwab et al. 2016). In our study, trichome density was reduced by Ag-NPs on the abaxial leaf surface of foliar treatment oaks. Although we did not characterize the chemical composition of organic compounds of leaf tissues, the organic composition of leaf structures might electrostatically bind the NPs, which, in turn, could be internalized into leaf tissues and translocated to other tissues (Hong et al. 2014).

Although the processes involved in the translocation of NPs within trees through leaf uptake remain to be investigated more thoroughly, we found a greater amount of Ag in the stem of foliar treatment trees than in root treatment trees. Thus, we

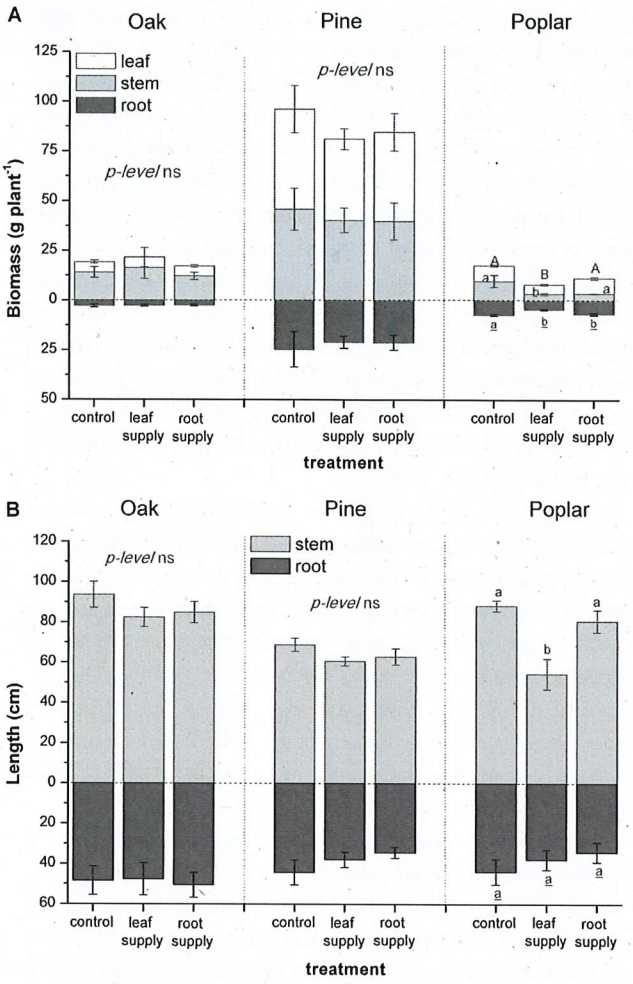

Figure 2. Leaf, stem and root biomass (DW, g) (A) and stem and root length (cm) (B) of oak, pine and poplar plants exposed to control, foliar and root treatments. The values are the mean ± SD ($n = 5$). Different letters represent statistical differences between treatments within tissues (capital letter for leaf; lowercase letters for stem; underlined letters for root) (Tukey-HSD multiple comparisons at $P < 0.05$ level).

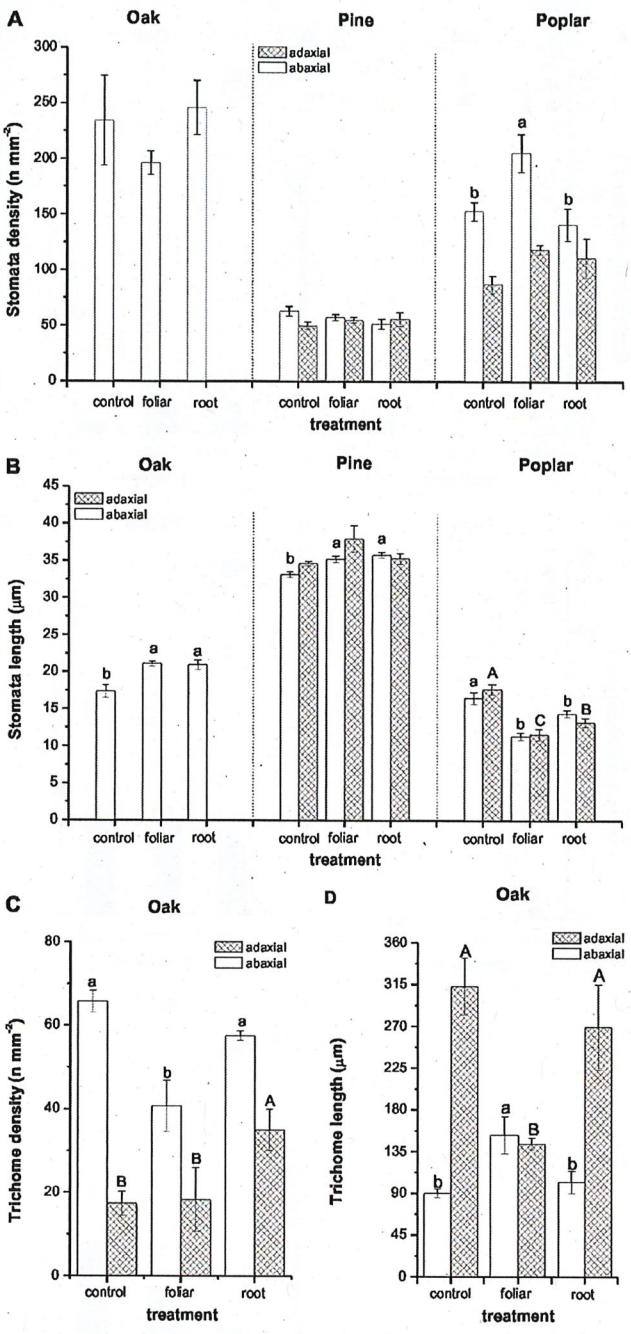

Figure 3. Stomatal density (A) and length (B) of adaxial and abaxial leaf surfaces in oak, pine and poplar; trichome density (C) and length (D) in oak leaves exposed to control, foliar and root treatments. The values are the mean ± SD ($n = 5$). Different letters represent statistical differences between treatments within tissues (lowercase letters for abaxial leaf surface; capital letters for adaxial leaf surface) (Tukey-HSD multiple comparisons at $P < 0.05$ level).

observed that NPs are transported from leaves to the stem as photosynthates, most probably via phloem, confirming previous observations (Shahid et al. 2017). Such processes are affected by metabolic activity, as shown by Zhai et al. (2014) for poplar, in which Au-NPs were found to be transported from one cell to another through plasmodesmata. The mechanisms by which NPs are transported into plant cells is not well understood and can be limited by the pore size of cell walls (2–20 nm; Zhai et al. 2014).

Effects Ag-NPs on plant traits

Foliar application of Ag-NPs decreased plant growth, above-ground biomass and stem length in poplar. In contrast, no such effects were found in oak and pine (Figure 2), probably because of the greater translocation efficiency, faster plant growth and higher gas exchange of these species (Robinson et al. 2000). Lower biomass and stem lengths in foliar treatment poplars in comparison with root treatment and control trees corresponded to higher Ag concentrations in stem tissue. The

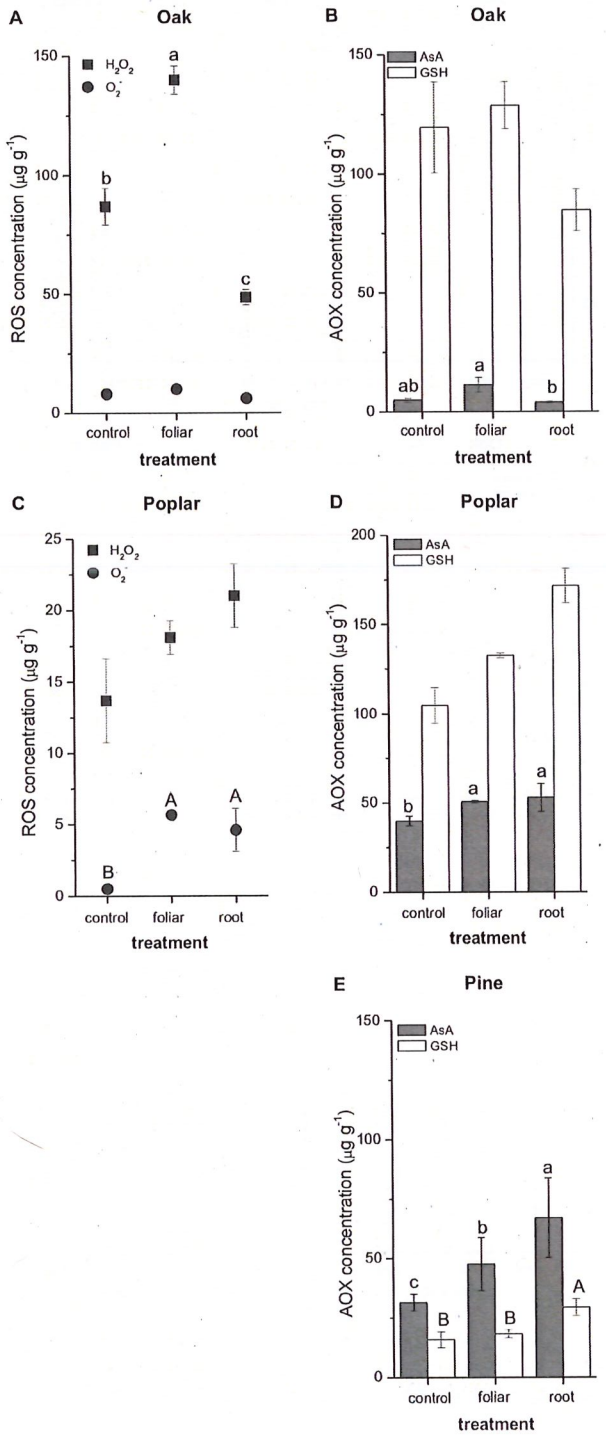

Figure 4. Reactive oxygen species (ROS) (hydrogen peroxide, H_2O_2; superoxide anion, O_2^-) and AOX (ascorbic acid, AsA; glutathione, GSH) in leaves of oak (A and B), poplar (C and D) and pine (E) plants exposed to control, foliar and root treatments. The values are the mean ± SD ($n = 5$). Different letters represent statistical differences between treatments for each compound (lowercase letters for AsA and H_2O_2; capital letters for GSH and O_2^-) (Tukey-HSD multiple comparisons at $P < 0.05$ level).

concentration of NPs supplied to oak and pine in this experiment was lower than that considered as phytotoxic, e.g., 350 and 790 mg kg^{-1} by Sweet and Singleton (2015) for Bishop pine, but higher than the 50 ppm found to be toxic for English oak (Olchowik et al. 2017). The permeability of leaves may also play a role in explaining such differences and may be particularly relevant for poplar considering the structural traits of poplar leaves in comparison with those of oak and pine (Sweet and Singleton 2015, Olchowik et al. 2017). Moreover, the biomass of foliar treatment poplars decreased, whereas it increased that of photoassimilating organs in comparison with control trees. This finding supports the 'optimal partitioning theory', which suggests that higher biomass is allocated to leaves if environmental disturbances come from aboveground and vice versa (Gedroc et al. 1996).

The supply of Ag-NPs induced significant changes in leaf traits, specifically the increased stomatal density and decreased stomatal length in poplar, the low trichome density and trichome length in oak. These may represent compensatory mechanisms to balance gas exchange or an adaptive strategy to modulate assimilation surfaces in response to stress conditions (e.g., Marchi et al. 2008). Phenotypic plasticity of leaf structures changes in response to environment following defensive adaptation strategies, such as the storage of NPs to detox plant tissues (Cifuentes et al. 2010).

Photosynthetic capacity was not clearly affected by Ag-NPs. However, the young and efficient photosynthetic tissues (Marcelis 1996), as well as the plastic structural (leaf structures and 'C/F') and biochemical (antioxidant system) traits, might have favored physiological adjustments (Peng and Gong 2014, Regier et al. 2014, Xiong et al. 2017). The supply of NPs decreased progressively J_{max} in root treatment oaks and in foliar treatment pines, pointing to somewhat stressful conditions (Sperlich et al. 2016). Conversely, by the end of the experiment, poplar was able to optimize resource allocation relatively well to preserve a balance between enzymatic (Rubisco) and light-harvesting (chlorophyll) capabilities across treatments (Tognetti et al. 2004). The sensitivity of simulated carboxylation rates to variations in Vc_{max} and J_{max} suggests a response to Ag-NPs (Xiong et al. 2016), although photosynthetic gain and the costs of energy dissipation were not affected. Dynamic responses of Vc_{max} and J_{max} indicate that the photosynthetic system has leaf-level capacities to adjust optimally to environmental variability and resource supply (Quebbeman and Ramirez 2016).

Oak and poplar produced ROS when supplied with NPs, and this may stimulate the scavenging system (Di Baccio et al. 2009). In particular, foliar treatment oaks accumulated H_2O_2, whereas higher O_2^- was found in both foliar treatment and root treatment poplars, and pines did not produce ROS. In this study, the production of ROS was accompanied by the synthesis of AsA in oaks and GSH in poplars supplied with Ag-NPs. This process activated antioxidant mechanisms involved in the

protection of plant tissues from oxidative stress, maintaining vital physiological activities. Moreover, although ROS was not detected in pine, AOX were produced, suggesting that ROS could be quickly detoxified. Conversely, the antioxidant activity in pine needles could be attributed to the high content of aromatic and phenolic compounds preventing the decomposition of peroxides and free radical scavenging activities (Jia et al. 2010, Leopoldini et al. 2011, Zeng et al. 2012).

Consequences of Ag-NPs on microbial populations

Microbial populations were affected by the foliar treatment, with a reduction in the survival of bacteria (oak and poplar) and fungi (pine). Silver ions accumulate in the bacterial cytoplasm and result in membrane disruption and alterations in the integrity of cells (Tripathi et al. 2017). Root treatment exhibited changes in the root bacterial populations in poplar, confirming the sensitivity and plasticity of this species in response to environmental changes (Tognetti et al. 2013). An unexpected increase in fungal population was detected on the roots of poplars, colonized by *Trichoderma* spp. that may have inhibited the growth of other fungi. Olchowik et al. (2017) observed that the degree of mycorrhization increased significantly in English oak seedlings treated with Ag-NPs at concentrations 25 ppm, in comparison with other doses of Ag-NPs supplied to plants. Microbial communities influence the metal dissolution in the substrate and the availability of metals or metalloids in trees (Bravin et al. 2012, Rajkumar et al. 2012) through the excretion of various inorganic and organic compounds (Lindow and Brandl 2003) or the acidification of the environment (Ma et al. 2011). Assessments of microbial colonization in plant-polluted systems, therefore, may provide useful information on the tolerance mechanisms of plant–microbe systems to pollutants, as well as on the choice of suitable phytotechnologies to mitigate environmental risks due to contaminant exposure (Cocozza et al. 2014, 2015).

Conclusions

Our experiment demonstrates that Ag-NPs enter into the stem through leaves faster than through roots. Nanoparticles may accumulate in woody tissues once transported through the vascular system (Seeger et al. 2009, Schreck et al. 2014, Shahid et al. 2017), although the role of foliar versus root uptake in element speciation, toxicity, compartmentation and detoxification in trees needs further investigation. Since the availability of pollutants at root level represents a minor transfer pathway of NPs compared with foliar uptake, a thorough understanding of the effects of NPs on species-specific assimilation processes and growth traits is critical for a careful evaluation of their impacts on trees in the urban environment.

Conflict of interest

None declared.

Authors' contributions

C.C., R.T. and P.C. planned and designed the research. A.P., C.G., M.C.S., S.P., A.R., M.S. and K.S. performed experiments, conducted fieldwork and analyzed the data. C.C., A.P., J.L.I., R.T. and P.C. wrote the manuscript.

References

Alexieva V, Sergiev I, Mapelli S, Karanov E (2001) The effect of drought and ultraviolet radiation on growth and stress markers in pea and wheat. Plant Cell Environ 24:1337–1344.

Barrena R, Casals E, Colón J, Font X, Sánchez A, Puntes V (2009) Evaluation of the ecotoxicity of model nanoparticles. Chemosphere 75:850–857.

Birbaum K, Brogioli R, Schellenberg M, Martinoia E, Stark WJ, Günther D, Limbach LK (2010) No evidence for cerium dioxide nanoparticle translocation in maize plants. Environ Sci Technol 44:8718–8723.

Bravin MN, Garnier C, Lenoble V, Gérard F, Dudal Y, Hinsinger P (2012) Root-induced changes in pH and dissolved organic matter binding capacity affect copper dynamic speciation in the rhizosphere. Geochim Cosmochim Acta 84:256–268.

Cifuentes Z, Custardoy L, de la Fuente JM, Marquina C, Ibarra MR, Rubiales D, Pérez-de-Luque A (2010) Absorption and translocation to the aerial part of magnetic carbon-coated nanoparticles through the root of different crop plants. J Nanobiotechnology 8:26.

Cocozza C, Trupiano D, Lustrato G et al. (2015) Challenging synergistic activity of poplar–bacteria association for the Cd phytostabilization. Environ Sci Pollut Res 22:19546–19561.

Cocozza C, Vitullo D, Lima G, Maiuro L, Marchetti M, Tognetti R (2014) Enhancing phytoextraction of Cd by combining poplar (clone "I-214") with *Pseudomonas fluorescens* and microbial consortia. Environ Sci Pollut Res 21:1796–1808.

Cutter BE, Guyette RP (1993) Anatomical, chemical and ecological factors affecting tree species choice in dendrochemistry studies. J Environ Qual 22:611–619.

Di Baccio D, Tognetti R, Minnocci A, Sebastiani L (2009) Responses of the *Populus* × *euramericana* clone I-214 to excess zinc: carbon assimilation, structural modifications, metal distribution and cellular localization. Environ Exp Bot 67:153–163.

Dietz KJ, Herth S (2011) Plant nanotoxicology. Trends Plant Sci 16:582–589.

Dimkpa CO, McLean JE, Martineau N, Britt DW, Haverkamp R, Anderson AJ (2013) Silver nanoparticles disrupt wheat (*Triticum aestivum* L.) growth in a sand matrix. Environ Sci Technol 47:1082–1109.

Eichert T, Kurtz A, Steiner U, Goldbach HE (2008) Size exclusion limits and lateral heterogeneity of the stomatal foliar uptake pathway for aqueous solutes and water suspended nanoparticles. Physiol Plant 134:151–160.

Eisler R (1997) Silver hazards to fish, wildlife and invertebrates: a synoptic review. US Department of the Interior, National Biological Service, Washington, DC, 44 p. (Biological Report 32 and Contaminant Hazard Reviews Report 32).

Elstner EF, Heupel A (1976) Inhibition of nitrate formation from hydroxylammoniumchloride: a simple assay for superoxide dismutase. Anal Biochem 70:616–620.

El-Temsah YS, Joner EJ (2012) Impact of Fe and Ag nanoparticles on seed germination and differences in bioavailability during exposure in aqueous suspension and soil. Environ Toxicol 27:42–49.

Feldmann J, Raab A, Krupp EM (2018) Importance of ICPMS for speciation analysis is changing: future trends for targeted and non-targeted element speciation analysis. Anal Bioanal Chem 410: 661–667.

Gedroc JJ, Mcconnaughay KDM, Coleman JS (1996) Plasticity in root/shoot partitioning: optimal, ontogenetic, or both? Funct Ecol 10:44–50.

Hong J, Peralta-Videa JR, Rico C, Sahi S, Viveros MN, Bartonjo J, Zhao L, Gardea-Torresdey JL (2014) Evidence of translocation and physiological impacts of foliar applied CeO_2 nanoparticles on cucumber (*Cucumis sativus*) plants. Environ Sci Technol 48:4376–4385.

Howe PD, Dobson S (2002) Silver and silver compounds: environmental aspects, Concise international chemical assessment document, 44. World Health Organization, Geneva, Switzerland.

Hull HM, Morton HL, Wharrie JR (1975) Environmental influences on cuticle development and resultant foliar penetration. Bot Rev 41:421–452.

Jia HL, Ji QL, Xing SL, Zhang PH, Zhu GL, Wang XH (2010) Chemical composition and antioxidant, antimicrobial activities of the essential oils of *Thymus marschallianus* Will. and *Thymus proximus* Serg. J Food Sci 75:E59–E65.

Jiang M, Zhang J (2001) Effect of abscissic acid on active oxygen species, antioxidative defence system and oxidative damage in leaves of maize seedlings. Plant Cell Physiol 42:1265–1273.

Kim SW, Jung JH, Lamsal K, Kim YS, Min JS, Lee YS (2012) Antifungal effect of silver nanoparticles (AgNPs) against various plant pathogenic fungi. Mycobiology 40:53–58.

Kim HS, Oren R, Hinckley TM (2008) Actual and potential transpiration and carbon assimilation in an irrigated poplar plantation. Tree Physiol 28:559–577.

Larue C, Castillo-Michel H, Sobanska S, Cécillon L, Bureau S, Barthès V, Ouerdane L, Carrière M, Sarret G (2014) Foliar exposure of the crop *Lactuca sativa* to silver nanoparticles: evidence for internalization and changes in Ag speciation. J Hazard Mater 264:98–106.

Law MY, Charles SA, Halliwell B (1983) Glutathione and ascorbic acid in spinach (*Spinacea oleracea*) chloroplasts. The effect of hydrogen peroxide and of Paraquat. J Biochem 210:899–903.

Lee W, An Y, Yoon H, Kweon H (2008) Toxicity and bioavailability of copper nanoparticles to the terrestrial plants mung bean (*Phaseolus radiatus*) and wheat (*Triticum aestivum*): plant uptake for water insoluble nanoparticles. Environ Toxicol Chem 27:1915–1921.

Leopoldini M, Russo N, Toscano M (2011) The molecular basis of working mechanism of natural polyphenolic antioxidants. Food Chem 125:288–306.

Li Q, Li Y, Zhu L, Xing B, Chen B (2017) Dependence of plant uptake and diffusion of polycyclic aromatic hydrocarbons on the leaf surface morphology and micro-structures of cuticular waxes. Sci Rep 7:46235.

Lin D, Xing B (2007) Phytotoxicity of nanoparticles: inhibition of seed germination and root growth. Environ Pollut 150:243–250.

Lindow SE, Brandl MT (2003) Microbiology of the phyllosphere. Appl Environ Microbiol 69:1875–1883.

Ma X, Geiser-Lee J, Deng Y, Kolmakov A (2010) Interactions between engineered nanoparticles (ENPs) and plants: phytotoxicity, uptake and accumulation. Sci Tot Environ 408:3053–3061.

Ma Y, He X, Zhang P et al. (2011) Phytotoxicity and biotransformation of La_2O_3 nanoparticles in a terrestrial plant cucumber (*Cucumis sativus*). Nanotoxicology 5:743–753.

Maillard JY, Hartemann P (2012) Silver as an antimicrobial: facts and gaps in knowledge. Crit Rev Microbiol 39:373–383.

Marcelis LFM (1996) Sink strength as a determinant of dry matter partitioning in the whole plant. J Exp Bot 47:1281–1291.

Marchi S, Tognetti R, Minnocci A, Borghi M, Sebastiani L (2008) Variation in mesophyll anatomy and photosynthetic capacity during leaf development in a deciduous mesophyte fruit tree (*Prunus persica*) and in evergreen sclerophyllous Mediterranean shrub (*Olea europea*). Trees 22:559–571.

Monsi M, Saeki T (2005) On the factor light in plant communities and its importance for matter production. Ann Bot 95:549–567.

Nair R, Varghese SH, Nair BG, Maekawa T, Yoshida Y, Kumar DS (2010) Nanoparticulate material delivery to plants. Plant Sci 179: 154–163.

Navarro E, Baun A, Behra R, Hartmann NB, Filser J, Miao AJ, Quigg A, Santschi PH, Sigg L (2008) Environmental behavior and ecotoxicity of engineered nanoparticles to algae, plants, and fungi. Ecotoxicology 17:372–386.

Nel A, Xia T, Mädler L, Li N (2006) Toxic potential of materials at the nanolevel. Science 311:622–627.

Nowack B, Bucheli TD (2007) Occurrence, behavior and effects of nanoparticles in the environment. Environ Pollut 150:5–22.

OECD (2010) Organisation for Economic Co-operation and Development. Guidance manual for the testing of manufactured nanomaterials. http://www.oecd.org/env/ehs/nanosafety/publications-series-safety-manufactured-nanomaterials.htm.

Okamura M (1980) An improved method for determination of L-ascorbic acid and L-dehydroascorbic acid in blood plasma. Clin Chim Acta 103:259–268.

Olchowik J, Bzdyk RM, Studnicki M, Bederska-Błaszczyk M, Urban A, Aleksandrowicz-Trzcińska M (2017) The effect of silver and copper nanoparticles on the condition of English Oak (*Quercus robur* L.) seedlings in a container nursery experiment. Forests 8:310.

Peng JS, Gong JM (2014) Vacuolar sequestration capacity and long-distance metal transport in plants. Front Plant Sci 5:1–5.

Percy KE, Cape J, Jagels R, Simpson CJ (2013) Air pollutants and the leaf cuticle, Vol. 36. Springer Science & Business Media, Berlin, Germany.

Quebbeman JA, Ramirez JA (2016) Optimal allocation of leaf-level nitrogen: implications for covariation of V_{cmax} and J_{cmax} and photosynthetic downregulation. J Geophys Res Biogeosci 121:2464–2475.

Rajkumar M, Sandhya S, Prasad MN, Freitas H (2012) Perspectives of plant-associated microbes in heavy metal phytoremediation. Biotechnol Adv 30:1562–1574.

Raliya R, Franke C, Chavalmane S, Nair R, Reed N, Biswas P (2016) Quantitative understanding of nanoparticle uptake in watermelon plants. Front Plant Sci 7:1288.

Regier N, Cosio C, von Moos N, Slaveykova VI (2014) Effects of copper-oxide nanoparticles, dissolved copper and ultraviolet radiation on copper bioaccumulation, photosynthesis and oxidative stress in the aquatic macrophyte *Elodea nuttallii*. Chemosphere 128: 56–61.

Regier N, Streb S, Cocozza C, Schaub M, Cherubini P, Zeeman SC, Frey B (2009) Drought tolerance of two black poplar (*Populus nigra* L.) clones: contribution of carbohydrates and oxidative stress defence. Plant Cell Environ 32:1724–1736.

Rico CM, Majumdar S, Duarte-Gardea M, Peralta-Videa JR, Gardea-Torresdey JL (2011) Interaction of nanoparticles with edible plants and their possible implications in the food chain. J Agric Food Chem 59:3485–3498.

Robinson BH, Mills TM, Petit D, Fung LE, Green SR, Clothier BE (2000) Natural and induced cadmium-accumulation in poplar and willow: implications for phytoremediation. Plant Soil 227:301–306.

Samberg ME, Orndorff PE, Monteiro-Riviere NA (2011) Antibacterial efficacy of silver nanoparticles of different sizes, surface conditions and synthesis methods. Nanotoxicology 5:244–253.

Schaad NW, Jones JB, Chum W (2001) Laboratory guide for identification of plant pathogenic bacteria, 3rd edn. APS Press, St Paul, MN, USA.

Schreck E, Dappe V, Sarret G et al. (2014) Foliar or root exposures to smelter particles: consequences for lead compartmentalization and speciation in plant leaves. Sci Total Environ 476–477: 667–676.

Schwab F, Zhai G, Kern M, Turner A, Schnoor JL, Wiesner MR (2016) Barriers, pathways and processes for uptake, translocation and accumulation of nanomaterials in plants—critical review. Nanotoxicology 10:257–278.

Sedlak J, Lindsay RH (1968) Estimation of total, protein-bound and nonprotein sulfhydryl groups in tissue with Ellman's reagent. Anal Biochem 25:192–205.

Seeger EM, Baun A, Kästner M, Trapp S (2009) Insignificant acute toxicity of TiO_2 nanoparticles to willow trees. J Soils Sediments 9:46–53.

Sgrigna G, Sæbø A, Gawronski S, Popek R, Calfapietra C (2015) Particulate matter deposition on *Quercus ilex* leaves in an industrial city of Central Italy. Environ Pollut 197:187–194.

Shahid M, Austruy A, Echevarria G, Arshad M, Sanaullah M, Aslam M, Nadeem M, Jatoi WN, Dumat C (2014) EDTA-enhanced phytoremediation of heavy metals: a review. Soil Sediment Contam 23:389–416.

Shahid M, Dumat C, Khalid S, Schreck E, Xiong T, Niazi NK (2017) Foliar heavy metal uptake, toxicity and detoxification in plants: a comparison of foliar and root metal uptake. J Hazard Mater 325:36–58.

Sharkey TD, Bernacchi CJ, Farquhar GD, Singsaas EL (2008) Fitting photosynthetic carbon dioxide response curves for C3 leaves. Plant Cell Environ 30:1035–1040.

Smita S, Gupta SK, Bartonova A, Dusinska M, Gutleb AC, Rahman Q (2012) Nanoparticles in the environment: assessment using the causal diagram approach. Environ Health 11:S13.

Sperlich D, Barbeta A, Ogaya R, Sabaté S, Peñuelas J (2016) Balance between carbon gain and loss under long-term drought: impacts on foliar respiration and photosynthesis in *Quercus ilex* L. J Exp Bot 67:821–833.

Sweet MJ, Singleton I (2015) Soil contamination with silver nanoparticles reduces Bishop pine growth and ectomycorrhizal diversity on pine roots. J Nanopart Res 17:448.

Tognetti R, Cocozza C, Marchetti M (2013) Shaping the multifunctional tree: the use of Salicaceae in environmental restoration. iForest 6:37–47.

Tognetti R, Sebastiani L, Minnocci A (2004) Gas exchange and foliage characteristics of two poplar clones grown in soil amended with industrial waste. Tree Physiol 24:75–82.

Tripathi DK, Tripathi A, Shweta SS et al. (2017) Uptake, accumulation and toxicity of silver nanoparticle in autotrophic plants, and heterotrophic microbes: a concentric review. Front Microbiol 8:7.

Ugolini F, Tognetti R, Raschi A, Bacci L (2013) *Quercus ilex* L. as bioaccumulator for heavy metals in urban areas: effectiveness of leaf washing with distilled water and considerations on the trees distance from traffic. Urban For Urban Green 12:576–584.

Wang J, Koo Y, Alexander A et al. (2013) Phytostimulation of poplars and *Arabidopsis* exposed to silver nanoparticles and Ag+ at sublethal concentrations. Environ Sci Technol 47:5442–5449.

Wang W, Tarafdar J, Pratim B (2013) Nanoparticle synthesis and delivery by an aerosol route for watermelon plant foliar uptake. J Nanopart Res 15:1417–1418.

Wang P, Lombi E, Zhao FJ, Kopittke PM (2016) Nanotechnology: a new opportunity in plant sciences. Trends Plant Sci 21:699–712.

Xiong T, Austruy A, Pierart A, Shahid M, Schreck E, Mombo S, Dumat C (2016) Kinetic study of phytotoxicity induced by foliar lead uptake for vegetables exposed to fine particles and implications for sustainable urban agriculture. J Environ Sci 46:16–27.

Xiong T, Dumat C, Dappe V, Vezin H, Schreck E, Shahid M, Pierart A, Sobanska S (2017) Copper oxide nanoparticle foliar uptake, phytotoxicity, and consequences for sustainable urban agriculture. Environ Sci Technol 51:5242–5251.

Yang F, Hong F, You W, Liu C, Gao F, Wu C, Yanng P (2006) Influences of nano-anatase TiO_2 on the nitrogen metabolism of growing spinach. Biol Trace Elem Res 110:179–190.

Yin L, Colman BP, McGill BM, Wright JP, Bernhardt ES (2012) Effects of silver nanoparticle exposure on germination and early growth of eleven wetland plants. PLoS One 7:e47674.

Zeng WC, Zhang Z, Gao H, Jia LR, He Q (2012) Chemical composition, antioxidant, and antimicrobial activities of essential oil from pine needle (*Cedrus deodara*). J Food Sci 77:C824–C829.

Zhai G, Walters KS, Peate DW, Alvarez PJJ, Schnoor JL (2014) Transport of gold nanoparticles through plasmodesmata and precipitation of gold ions in woody poplar. Environ Sci Technol Lett 1: 146–151.